Mobility of Adsorbed Proteins: A Brownian Dynamics Study

S. Ravichandran and J. Talbot
Department of Chemistry and Biochemistry, Duquesne University, Pittsburgh, Pennsylvania 15282 USA

ABSTRACT We simulate the adsorption of lysozyme on a solid surface, using Brownian dynamics simulations. A protein molecule is represented as a uniformly charged sphere and interacts with other molecules through screened Coulombic and double-layer forces. The simulation starts from an empty surface and attempts are made to introduce additional proteins at a fixed time interval that is inversely proportional to the bulk protein concentration. We examine the effect of ionic strength and bulk protein concentration on the adsorption kinetics over a range of surface coverages. The structure of the adsorbed layer is examined through snapshots of the configurations and quantitatively with the radial distribution function. We extract the surface diffusion coefficient from the mean square displacement. At high ionic strengths the Coulombic interaction is effectively shielded, leading to increased surface coverage. This effect is quantified with an effective particle radius. Clustering of the adsorbed molecules is promoted by high ionic strength and low bulk concentrations. We find that lateral protein mobility decreases with increasing surface coverage. The observed trends are consistent with previous theoretical and experimental studies.

INTRODUCTION

Protein adsorption to solid surfaces is an interesting and important phenomenon (Andrade and Hlady, 1986; Horbett and Brash, 1995; MacRitchie, 1978). It plays a major role in diverse areas ranging from biomaterials selection, through chromatographic applications, to enzyme-enhanced laundry detergents (Andrade, 1985). Although many experimental and theoretical methods have been used to study protein adsorption, a clear understanding has yet to emerge. The main reason for the lack of progress is the complex nature of proteins and their interactions with solid surfaces.

Most of the experimental studies indicate that protein adsorption is an irreversible process that leads to monolayer coverage (Ramsden, 1995; Schmitt et al., 1983). With recent advances in experimental techniques one can determine with precision the number density of adsorbed proteins (to about ± 70 molecules μm^2) (Ramsden and Prenosil, 1994). The experiments, however, cannot provide molecular-level mechanistic information about the adsorption process.

Modeling protein adsorption has also proved challenging. A variety of approaches, ranging from detailed molecular models (Lu and Park, 1990; Lu et al., 1991; Lim and Herron 1991) to mesoscopic models (Roth and Lenhoff, 1993; Oberholzer et al., 1997b), have been used. Detailed molecular approaches are in principle the most realistic and informative for the current problem, but they are computationally demanding. As a result, simulations have been limited to low surface coverages, and, even here, one must resort to approximations, such as omitting the solvent completely.

Received for publication 28 May 1999 and in final form 26 August 1999.
Address reprint requests to Dr. S. Ravichandran, Department of Chemistry and Biochemistry, Duquesne University, 600 Forbes Ave., Pittsburgh, PA 15282. Tel.: 412-396-1670; Fax: 412-396-5683; E-mail: ravi@space1.chemistry.duq.edu.

0006-3495/00/01/110/11 $2.00

Mesoscopic models based on random sequential adsorption (RSA) (Rényi 1958; Swendsen, 1981; Schaaf and Talbot, 1989a) provide a more accurate description of protein adsorption than does the Langmuir approach (Langmuir, 1918). The basic RSA model describes the irreversible adsorption of nonoverlapping particles that are immobile on the surface once adsorbed. According to the RSA model, there is a maximum surface coverage (jamming limit) beyond which further adsorption becomes impossible (54.7% coverage for spherical particles). Despite its simplicity, RSA has been successfully used to explain and understand many of the experimental results (Ramsden, 1993; Feder and Giaever, 1980). The basic RSA model has led to numerous extensions and improvements (Adamczyk et al., 1994; Tarjus et al., 1990; Oberholzer et al., 1997a). Still a drawback, even of the improved RSA models, is their failure to account accurately for particle-surface interactions and surface mobility.

Continuum models based on colloidal principles also eschew a detailed molecular description and do not consider the solvents explicitly. Derjaguin-Landau-Verway-Overbeek (DLVO) theory (Hunter, 1992; Verway and Overbeek, 1948) has been successfully applied to the study of protein adsorption based on the assumptions that the particles are rigid, spherically charged objects and their interactions with each other and with the surface (electrostatic, dispersion, and solvation forces) are pairwise and additive. The assumption of rigidity is justifiable if the native structure of the protein is not significantly altered by the protein-surface interactions. For example, hen egg white lysozyme (HEL), a compact globular protein, has the same structure in solution and on the adsorption surface (Kondo et al., 1991; Robeson and Tilton, 1996; Billsten et al., 1998). Studies also show that the other forms of lysozyme (T4 and human) show larger denaturation effects upon adsorption compared to HEL (Horsley et al., 1991; Billsten et al., 1998). Lenhoff et al., in a series of studies (Roth and Lenhoff, 1993;

Johnson et al., 1994; Roth et al., 1998), found that the charged spherical model works extremely well for the adsorption of hard proteins like HEL. Recently, Oberholzer et al. (1997b), using this model, studied HEL adsorption on mica with a combined grand canonical Monte Carlo (GCMC) and Brownian dynamics (BD) simulation procedure. Their results agree well with the available experimental data, showing that the colloidal approach to the modeling of hard proteins is a reasonable approximation.

Several experimental studies (Michaeli et al., 1980; Burghardt and Axelrod, 1981; Chan et al., 1997; Tilton et al., 1990a) have confirmed the mobility of adsorbed proteins. Protein adsorption experiments also report surface coverages that are significantly greater than the RSA jamming limit, providing indirect evidence for lateral mobility (Norde and Lyklema, 1978). Protein mobility plays an important role in several areas. For example, it enhances the reaction rate in enzyme catalysis and receptor-ligand binding (Tilton, 1998). In general, surface diffusion will result in more efficient packing compared to a situation in which the adsorbed particles are immobile.

If the protein-protein interactions are favorable, surface diffusion may also lead to clustering. Haggerty and Lenhoff (1993), using scanning tunneling microscopy (STM), observed that lysozyme adsorbed to graphite surfaces forms ordered arrays, with lattice spacings that depend on both the bulk protein and the salt concentrations. Experiments performed on a hydrophobic adsorption surface also report similar findings (Shibata and Lenhoff, 1992).

Ramsden et al. (1994) studied the adsorption of two different forms of cytochrome P450 adsorbing on lipid bilayer membranes. At high bulk concentrations they observed adsorption kinetic behavior consistent with the RSA model, while at sufficiently low bulk concentrations Langmuir-like kinetics emerged. The authors attributed this switch to surface clustering resulting from translational mobility in the low bulk concentration case.

Nygren and Stenberg (1990), using transmission electron microscopy (TEM), studied the kinetics of ferritin adsorption on a hydrophobic quartz grid. They found that the initial adsorption proceeds with the formation of molecular clusters. The fractal dimension of the clusters suggests that they are not formed by diffusion-limited aggregation. Instead Nygren and Stenberg proposed that some restructuring of the clusters takes place.

Relatively few theoretical studies have attempted to investigate the role of surface mobility. Ansell and Dickinson (1985) reported a BD study of coagulation kinetics using 49 spherical colloidal particles interacting with a DLVO potential. Only irreversible cluster formation was allowed, and the clusters were assumed to have no internal degrees of freedom. Tarjus et al. (1990) showed how to incorporate diffusion into a generalized RSA model, but the equations can only be solved at low coverages. Moreover, clustering is not possible in this class of hard particle models.

While both the experimental and theoretical studies demonstrate the importance of lateral mobility under appropriate conditions, the following questions remain unanswered. First, how does lateral diffusion affect the surface coverage and adsorption kinetics? Second, what is the structure of the adsorbed layer that results from surface diffusion, and how does it depend on the ionic strength and bulk concentration?

Although a number of numerical studies have attempted to understand the role of hydrodynamic interactions in adsorption (Bafaluy et al., 1993; Pagonabarraga and Rubi, 1994), the influence of surface diffusion has been totally neglected.

Here we present a simulation study of lysozyme at a solid interface. The effect of lateral diffusion on the adsorption kinetics and structure of the adsorbed layer are investigated. The bulk protein concentration and the ionic strength are the independent variables. We show that the presence of surface diffusion does influence the adsorption kinetics and leads to cluster formation at high salt concentrations.

MODEL

In this work the hen egg white lysozyme molecules are modeled as charged spheres. Based on the experimental studies, the net charge (Z) on the protein is fixed as $+8$ (Roth and Lenhoff, 1993; Oberholzer et al., 1997b). The particle-particle interactions are modeled using the ideas of colloidal chemistry: the effect of solvent plus ions is taken into account, using a continuum approach through the ionic strength and dielectric constant.

The pair potential is a sum of electrostatic, van der Waals, and repulsive contributions:

$$U_{pp} = U^{el} + U^{vdw} + U^{rep} \tag{1}$$

The electrostatic contribution depends on the ionic strength, I, of the solution. The functional forms of these contributions are taken from Oberholzer et al. (Oberholzer et al., 1997b) and are given in Appendix A. Note that the potential form is based on continuum models and does not have a rigorous theoretical basis. Three widely different ionic strengths were chosen to study how these affect the adsorption kinetics (see Fig. 1). This plot shows that the interaction is highly repulsive at short distances, attractive at intermediate distances, and negligible at large distances. The figure also shows that the intermediate minimum is preceded by a potential barrier. The barrier height (U^*) and its peak position (r^*) also depend on the ionic strength of the medium (see *inset* of Fig. 1).

SIMULATION PROCEDURE

A BD code has been developed to study protein adsorption to a surface. The simulations were performed in a square cell of side $L^* = L/a = 40$ with periodic boundary condi-

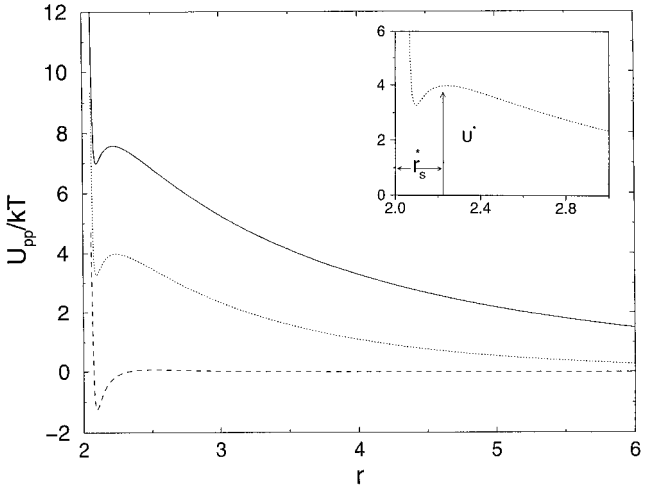

FIGURE 1 Pair potential used to model the lysozyme-lysozyme interaction for three different salt concentrations $I = 0.0015$ (*solid line*), 0.01 (*dotted line*), and 0.3 (*dashed line*). Note that r is scaled by the particle radius, a. *Inset*: Illustration of the barrier, U^*, in the pair potential. The ionic strength is $I = 0.01$ M.

tions. The potential was cut at a distance of $r_c^* = r_c/a$. The value of the r_c^* was chosen based on the choice of ionic strength (see Fig. 1). The BD algorithm (Ermak and McCammon, 1978) for updating the particle positions is given by

$$\mathbf{r}_i(t + \Delta t) = \mathbf{r}_i(t) + \frac{D_0}{k_B T}\mathbf{F}_i(t)\Delta t + \mathbf{R}_i(\Delta t) \qquad (2)$$

where $\mathbf{r}(t)$ denotes the position of the particle at time t, k_BT is the Boltzmann constant times the temperature, $\mathbf{F}_i$ is the total force acting on particle i, and Δt is the time step. D_0 is the lateral diffusion coefficient at zero coverage. The random displacement vectors, $\mathbf{R}_i$, are assumed to be normally distributed with zero mean and variance, given by $\langle \mathbf{R}_i \mathbf{R}_j \rangle = 2D_0\Delta t\delta_{ij}$, where δ_{ij} is the Kronecker delta.

The equations of motion were solved numerically with a reduced time step of $\Delta t^* = D_0\Delta t/a^2$, where a is the protein radius (1.5 nm for lysozyme). The value of D_0 was taken as 1×10^{-8} cm^2 s^{-1}, which is consistent with the experimentally available values (Tilton et al., 1990b). Usually simulations were performed for 10^7 Δt^*, where $\Delta L^* = 7 \times 10^{-6}$. The temperature of the system was 298 K, and the solvent was water with a dielectric constant of 80.

The overall simulation procedure has three steps:

1. Each simulation run is started from a bare adsorption surface.
2. An attempt is made to insert a new protein into the surface configuration, using an algorithm described below.
3. Irrespective of the outcome of the second step, BD simulation is performed on the adsorbed particles of the system. After every n_{ins} BD steps the simulation is interrupted and a new insertion attempt is made.
4. Steps 2 and 3 are repeated until the system saturates

Fig. 2 illustrates the different steps involved in the simulation. The results presented in this study were usually averaged over 40 separate runs. But the asymptotic coverages were calculated from the average of three individual runs.

In the absence of desorption, the adsorption kinetics can be described with an equation of the form

$$\frac{d\theta}{dt} = k_a c \Phi \qquad (3)$$

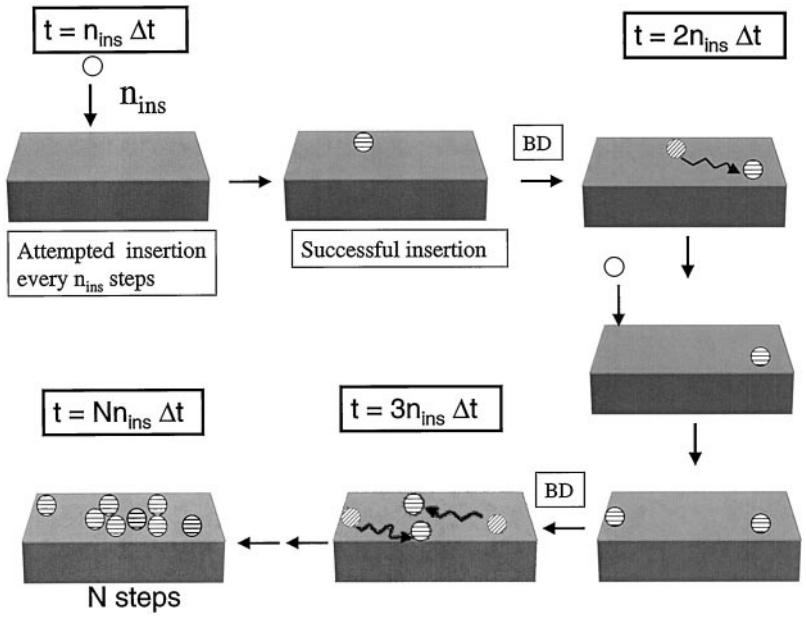

FIGURE 2 Schematic diagram of the different steps involved in the simulation. Spheres with slanted and straight design correspond, respectively, to the particle position before and after a period of BD simulation. The curved arrows show the path traversed by the particles during the BD simulation.

where $\theta = N\pi a^2/(L^2)$ is the coverage, N is the number of adsorbed particles, k_a is the adsorption rate constant, and c is the bulk concentration. The available surface function, Φ, represents the blocking effect of the adsorbed particles. The bulk concentration is inversely related to the insertion interval, n_{ins}. More specifically, one can show that (see Appendix B)

$$n_{ins} = \frac{\pi a^2}{L^2 \Delta t k_a c} \tag{4}$$

The algorithm for particle insertion is shown schematically in Fig. 3. The acceptance of a trial particle depends on its interaction energy with the rest of the system, U_{acc}. A trial particle is accepted with a probability $\exp(-U_{acc}/kT)$, where U_{acc} is essentially the maximum interaction of the trial particle with the remainder of the system as it approaches the surface. In some cases the maximum occurs when the particle reaches the surface, while in others the position of maximum energy is above the surface as the particle crosses a potential barrier. In this way one accounts for the fact that particles placed anywhere in the range of $2 < r < r_s^*$ (see Fig. 1) have to overcome the potential barrier U^*. So, in such cases it is the barrier height, rather than the total interaction energy, that is the deciding factor for particle acceptance. This choice also avoids particle clustering at the level of insertion. Particle-surface interactions are not explicitly included in our model. They play a major role, but under most conditions they can be regarded as a constant background and will not affect the adsorption kinetics.

The lateral diffusion coefficient and the insertion interval (n_{ins}) introduced earlier can be used to define the characteristic diffusion ($\tau_d = a^2/D_0$) and characteristic adsorption times ($\tau_a = [k_a c \Phi]^{-1}$), respectively (Schaaf and Talbot, 1989b). One can envisage two extreme situations:

1. The adsorbed particles diffuse rapidly on the surface. In such a case the characteristic diffusion time τ_d will be much smaller than the characteristic adsorption time. This situation corresponds very well to the low bulk protein concentration and low surface coverages.
2. The adsorbed particles are immobile on the adsorption surface. This situation can be described by a very large characteristic diffusion time compared to the adsorption time.

The effect of translational mobility on the adsorption kinetics can be studied by performing simulations with varying insertion interval n_{ins} values. A small value of n_{ins}, corresponding to a high bulk protein concentration, will tend to limit surface diffusion because of a rapid build-up of surface coverage. Three widely different values of n_{ins} (= 50, 1000, 2000) were chosen to study the effect of this parameter on the kinetics.

We also performed some runs using a larger adsorption surface [$(L^*)]^2 = 80 \times 80$)], where $L^* = L/a$ is the reduced cell side, and found that there is no significant system size effect compared with the (40 × 40) system used in this study.

RESULTS AND DISCUSSION

In Fig. 4, we present the kinetics for three different ionic strengths at $n_{ins} = 1000$. The results show that at a given time, the surface coverage increases with an increase in the salt concentration. A similar trend is seen with other n_{ins} (not shown). At high salt concentrations the net charge is effectively screened, leading to less repulsive protein-protein interactions, which allows a higher surface coverage. This behavior is reflected in the effective hard sphere radius r_{eff} (Adamczyk et al., 1994), chosen so that second virial coefficient of a hard disk fluid is the same as that of the

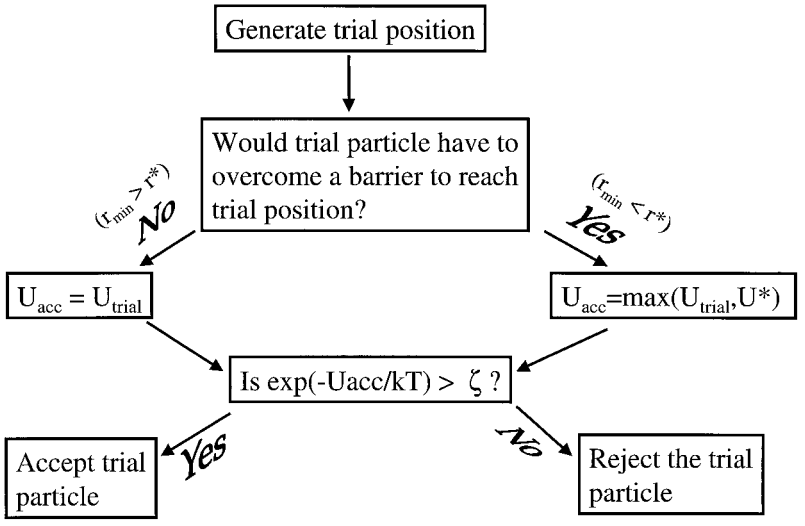

FIGURE 3 Particle insertion algorithm. U_{trial} is the energy of interaction of the trial particle with all adsorbed particles, r_{min} is the distance between the trial particle and its nearest neighbor, and U^* corresponds to the barrier height of the pair potential (see Fig. 1) at a reduced distance r^*. ζ is a uniformly distributed random number between 0 and 1.

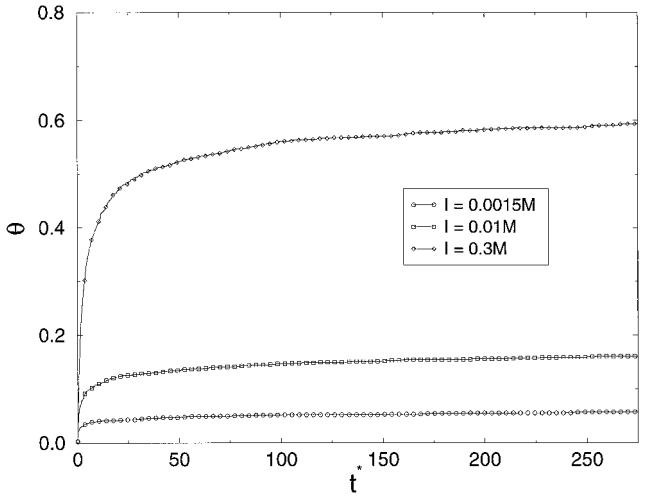

FIGURE 4 Plot of surface coverage against reduced time for three ionic strengths. The insertion interval is $n_{ins} = 1000$.

actual system. Specifically, the expression is

$$r_{eff}^2 = -1/2 \int_0^\infty (e^{-\beta U_{pp}(r)} - 1) r \, dr \tag{5}$$

where $\beta = 1/k_B T$, U_{pp} corresponds to the pair potential, and r is the reduced interparticle distance.

Fig. 5 shows a plot of the effective radius as a function of ionic strength. As the salt concentration decreases the effective radius increases, rapidly leading to more blocking, more repulsion, and less surface coverage. Note that the effective radius at the highest ionic concentration studied ($I = 0.3$ M) reduces to almost the radius of the particle. This essentially means that the particles can be more efficiently packed compared to the low salt concentration case. A similar trend has been observed for the adsorption of polyelectrolytes on silica surfaces (Bauer et al., 1998).

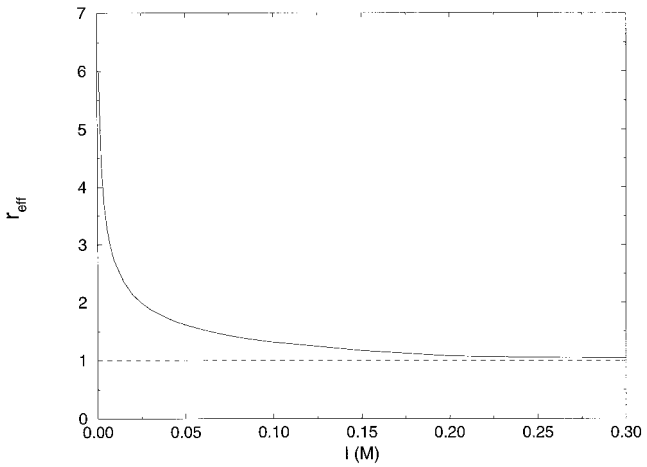

FIGURE 5 Effective radius (in units of a) as a function of ionic strength. The dashed line represents the particle radius.

The effect of translational mobility on the adsorption kinetics can be studied by comparing the kinetics at different insertion intervals. To make the comparison meaningful, we have introduced a scaled time defined by

$$t^* = k_a c t \tag{6}$$

This allows us not only to compare the results for different n_{ins}, but also to quantify the effect of lateral mobility on the adsorption kinetics.

The idea of time scaling can be understood by considering the RSA process. The kinetics of an irreversible adsorption process can be described by Eq. 3. For RSA, Φ is accurately represented by

$$\Phi(x) = \frac{(1-x)^3}{1 + a_1 x + a_2 x^2 + a_3 x^3} \tag{7}$$

where $x = \theta(r_{eff}^2/a^2)/\theta_\infty$, θ_∞ is the surface coverage at the jamming limit, $a_1 = -0.8120$, $a_2 = 0.2336$, and $a_3 = 0.0845$ (Schaaf and Talbot, 1989b). The time-dependent surface coverage can be computed by numerically integrating Eq. 3. In Fig. 6 we show the surface coverage as a function of time for a RSA process at three different arbitrary bulk concentrations ($\propto n_{ins}^{-1}$). After scaling, the individual curves corresponding to different bulk concentrations collapse onto a single curve. It is the absence of competing processes (e.g., translation or desorption) that results in this simple time scaling.

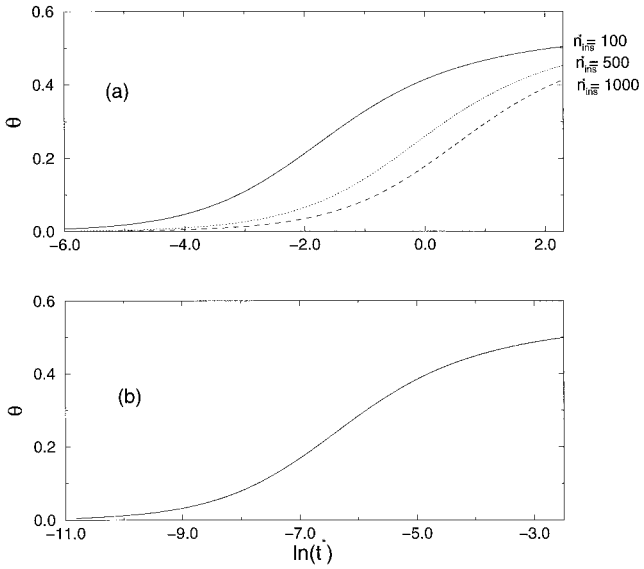

FIGURE 6 Plot illustrating the reduced time (a) time evolution of surface coverage of an RSA process for three different n_{ins}. These calculations were done for the adsorption surface length ($L^* = 40$) and correspond to $k_a c = 2.81$, 0.56, and 0.28, respectively. (b) Surface coverage against scaled time. Note that the three curves in a have collapsed into a single curve after scaling.

Fig. 7 shows the plot of surface coverage for $I = 0.3$ M against scaled time for different n_{ins}. It is clear that at a given time the surface coverage increases as n_{ins} increases. If lateral diffusion were insignificant, then one would expect the same coverage for different n_{ins}. But the different kinetic behavior in scaled time for different n_{ins} shows the importance of lateral diffusion, at least for this model. Why is the surface coverage for large n_{ins} more compared to the small n_{ins} case? The reason can be understood by the following argument. Small n_{ins} essentially means the characteristic adsorption time is much smaller than the diffusion time. If particles adsorb often (small n_{ins}), then the adsorbed particles will not move much on the surface before the arrival of new particles and the situation will be like that of RSA. On the other hand, if insertions are attempted less often (high n_{ins}), then the adsorbed particles have more time to diffuse, which partially relaxes an inefficiently packed configuration.

The effect of translational mobility on the adsorption kinetics can be better understood if we compare the results of the present simulation with the predictions of both the RSA and Langmuir models (see Fig. 7). Langmuir models are based on independent adsorption sites, and each molecule is assumed to interact only with one site. One can see that the Langmuir model agrees with the simulation results at very low surface coverage, and at higher coverages there is a considerable deviation. The RSA model predicts the lowest coverage at all times because of the absence of lateral diffusion.

One expects strong clustering to extend the range of validity of Langmuir theory because it is accompanied by an increase in the available surface. Moreover, if low bulk concentrations favor clustering, the Langmuir theory should provide a better description at higher n_{ins} (or low bulk concentrations), as was observed by Ramsden et al. (1994). We are not able to confirm this with the present model, perhaps because the clustering effect is not strong enough.

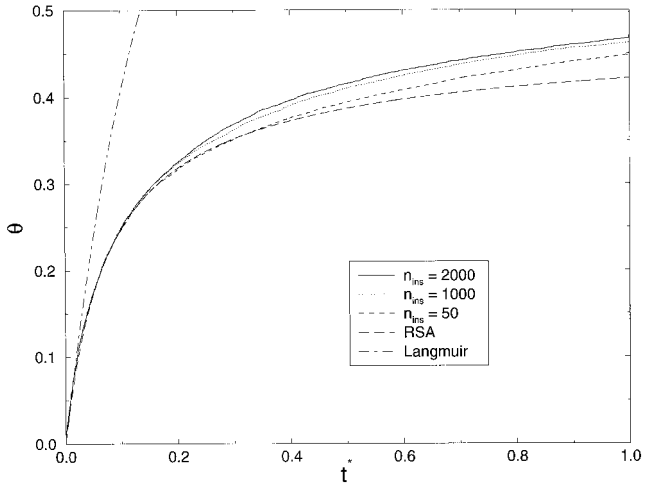

FIGURE 7 Surface coverage against scaled time for $I = 0.3$ M.

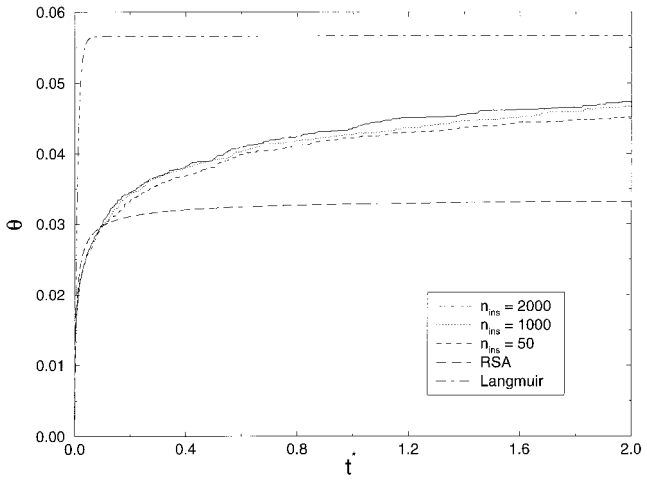

FIGURE 8 As in Fig. 9, except at $I = 0.0015$ M.

In Fig. 8 we plot the kinetics at low ionic strength ($I = 0.0015$ M). The trend is the same as at high ionic strength, but weaker. Based on the available results, we conclude that neither the RSA nor the Langmuir theory agrees with the simulation results. For example, RSA theory predicts the lowest coverage at all times for the different ionic strengths considered in this study, and the Langmuir theory overestimates the surface coverage. The reason for the difference between the simulation and the model predictions can be due to both the surface exclusion effects and the absence of lateral diffusion, the latter being the main focus of this study.

To quantify the structure of the adsorbed layer, we have computed the radial distribution function (RDF) of configurations close to saturation for different ionic strengths and n_{ins}. The RDF plot (Fig. 9) clearly shows that the highest ionic strength studied ($I = 0.3$ M) leads to the greatest

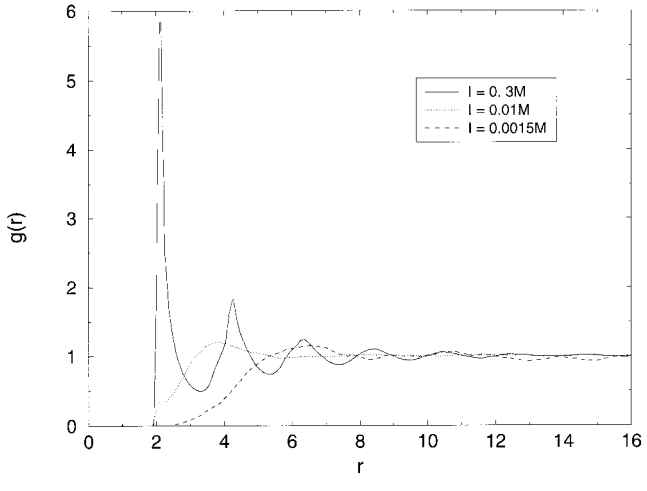

FIGURE 9 Radial distribution function as a function of particle particle separation, r, for three different ionic strengths and $n_{ins} = 1000$.

degree of local order. The same trend persists for other n_{ins} studied in this work. In Fig. 10 *a* we show the final configuration of one of the simulation runs for $I = 0.0015$ M, which shows no evidence of clustering. The configurations corresponding to other n_{ins} for $I = 0.0015$ M and $I = 0.01$ M are similar and are not shown. In Fig. 10, *b* and *c*, we show the configurations of the same number of particles at $I = 0.3$ M, for small and large insertion intervals. Unlike the low-ionic-strength case, there are some compact clusters as well as chains. Most significantly, these features are enhanced in the higher n_{ins} system (see Fig. 12). Configurations of intermediate coverage were intentionally chosen to show clearly the effect of translational mobility on the adsorption kinetics. It appears that at both high ionic strength and surface coverage the preformed smaller clusters coalesce to form bigger clusters, with the enhancement

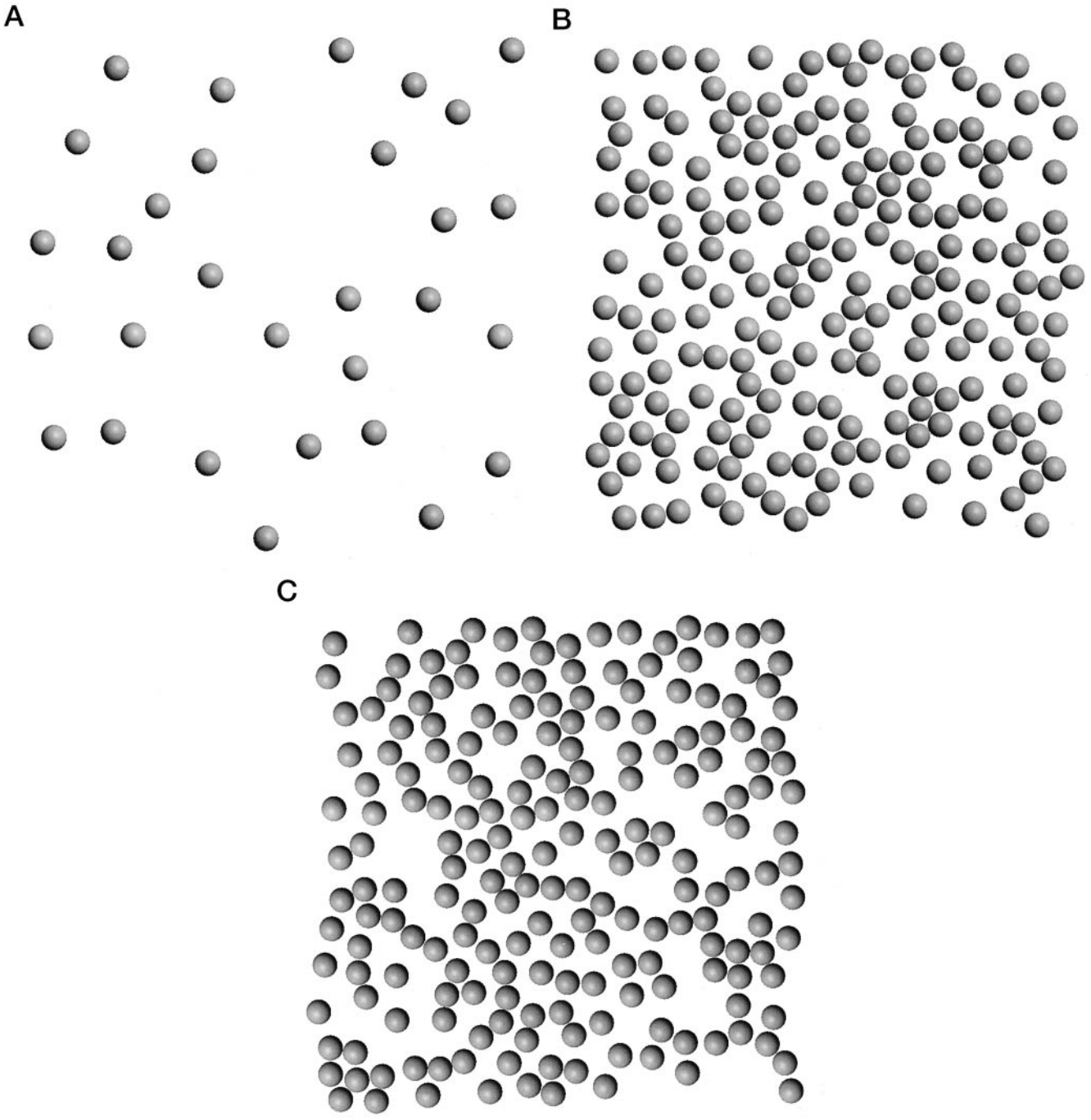

FIGURE 10 Simulation snapshot of the adsorbed particles at (*a*) $I = 0.0015$ M, $N = 30$, and $n_{ins} = 1000$; (*b*) $I = 0.3$ M, $N = 202$, and $n_{ins} = 50$; and (*c*) $I = 0.3$ M, $N = 202$, and $n_{ins} = 1000$.

in the chain length (see Fig. 11). Unlike the intermediate case, it is not easy to observe a difference in the structure of individual configurations at high concentrations for different n_{ins}. However, the difference in structure is evident from the RDFs, which are averaged over many configurations. The RDFs are also consistent with this observation in that the peaks are sharper and the minima deeper in the configurations with the larger insertion interval (see Fig. 12).

In both experiments and simulations the adsorption kinetics are typically very slow at long times. To estimate the saturation coverage, one must rely on a model prediction. RSA provides one limiting situation in which the adsorbed particles are immobile: in this case the surface coverage approaches the jamming limit, θ_∞, according to the power law form

$$\theta_\infty - \theta(t) = K/\sqrt{t} \tag{8}$$

where K is a constant (Pomeau, 1980; Swendsen, 1981). The other limit is provided by the work of Privman and Barma (1992), who studied the irreversible deposition kinetics of k-mers on a linear substrate. The limit $k \to \infty$ corresponds to rods adsorbing on a continuous surface. At long times the surface coverage evolves according to

$$\theta'_\infty - \theta(t) = K'[\ln(t)]^{-1}. \tag{9}$$

In Fig. 13 we compare the asymptotic surface coverage from simulations for three different salt concentrations, using this functional form. At long times the simulation results are indeed linear; the surface coverages in the jamming limit, obtained by extrapolating the results to infinite time, are shown in Table 1. The asymptotic value for $n_{ins} =$ 1000 is larger than $n_{ins} = 50$, in accord with the earlier results. The predicted values of the asymptotic coverage depend on the form selected for the asymptotic kinetics. Equation 9 follows from the assumption of fast surface diffusion, but it was derived for a 1D system, and it is not yet clear that a similar form applies in higher dimensions. We note that the maximum possible coverage for this model is 0.906, in all cases, corresponding to a hexagonal array of close-packed disks. To reach this state, however, a significant energy barrier must be overcome, particularly at low ionic strengths. One might reach this state, however, in the hypothetical case of infinitely long simulation.

We also fitted the simulation results to the power-law behavior predicted by RSA (Eq. 8). The long time fit is also reasonable, and the extrapolated coverages are, as expected,

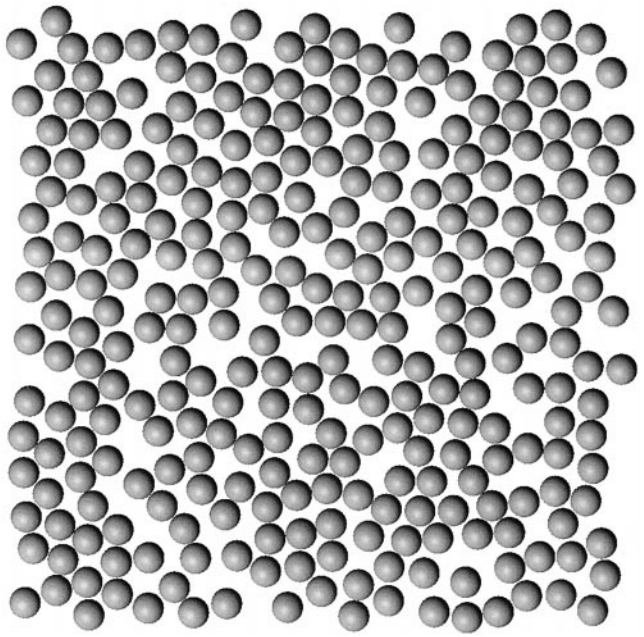

FIGURE 11 Simulation snapshot at $I = 0.3$ M, $N = 300$, and $n_{ins} = 50$.

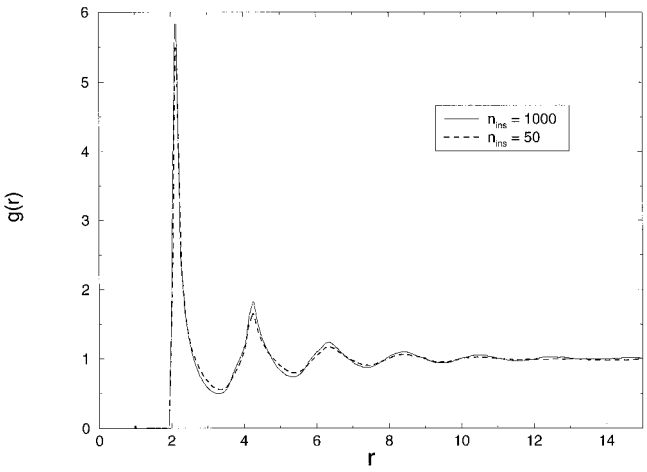

FIGURE 12 Comparison of radial distribution functions for $I = 0.3$ M.

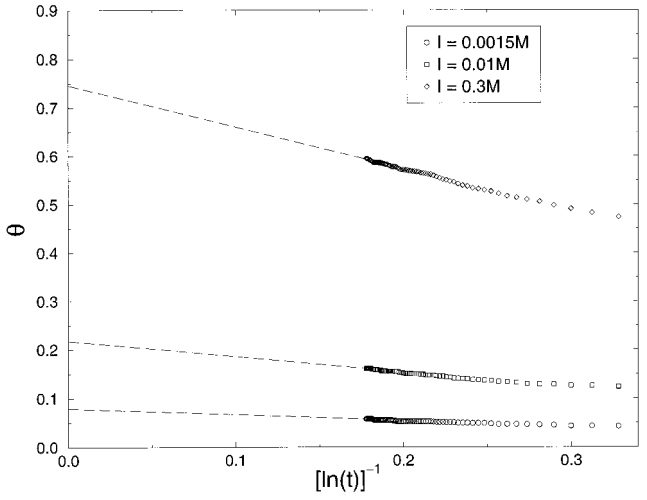

FIGURE 13 Surface coverage against $[\ln(t)]^{-1}$ for three different ionic strengths and $n_{ins} = 1000$. The dashed line shows the extrapolation to infinite time. Note that the results are obtained by averaging over three separate runs.

TABLE 1 Asymptotic surface coverage values from the simulation

n_{ins}	I = 0.0015 M	I = 0.01 M	I = 0.3 M
50	0.079	0.226	0.693
1000	0.082	0.236	0.744

The values are obtained by extrapolating the data in Fig. 13 to infinite time.

smaller than the corresponding values obtained by fitting Eq. 9. The RSA kinetics (Eq. 8) is specifically for the irreversible adsorption of spherical particles on a two-dimensional (planar) surface, but without surface diffusion.

We have also computed the lateral diffusion coefficients, D_T, via mean square displacement calculations. In Fig. 14 we plot the diffusion coefficients scaled by the zero surface coverage, D_0, against surface coverages for $I = 0.3$ M. The reason for choosing the high ionic strength is that significant coverages can be achieved, so that interaction effects can easily be observed. As expected, one can see that the diffusion coefficient of the particle decreases with increasing surface coverage.

Minton (1989) has proposed a simple model for the study of the effect of surface coverage on the lateral mobility of adsorbed proteins. The proteins are modeled as hard spheres and, using scaled particle theory (SPT), Minton obtained a simple analytic expression for the lateral diffusion coefficient,

$$D_T = D_0 e^{-[(y^2+4y)Q+(y^2+2y)Q^2]} \quad (10)$$

where y is the constant Brownian jump factor and $Q = \theta/(1 - \theta)$. The model predicts a decrease in the lateral diffusion with an increase in the adsorbed protein concentration. The reason for this behavior is attributed to the decrease in the probability of finding a vacancy in the immediate neighbor region. For $I = 0.3$ M we find the simulated value of y, or the average scaled distance the protein diffuses in one simulation step, to be 0.015. Fig. 14 shows the comparison of diffusion coefficients obtained from simulation and theory. The simulation result agrees qualitatively with the model for this value of y. The best fit of the model is obtained with a large value, $y = 0.07$ (see Fig. 14). It is not clear why the theory shows better agreement for a large Brownian displacement jump factor. But the SPT involves a number of assumptions, including that the close-packed coverage is unity (in reality, it is 0.906). The trends observed in the simulations are in accord with the available experimental (Tilton, 1998) and theoretical studies (Pink, 1985; Minton, 1989).

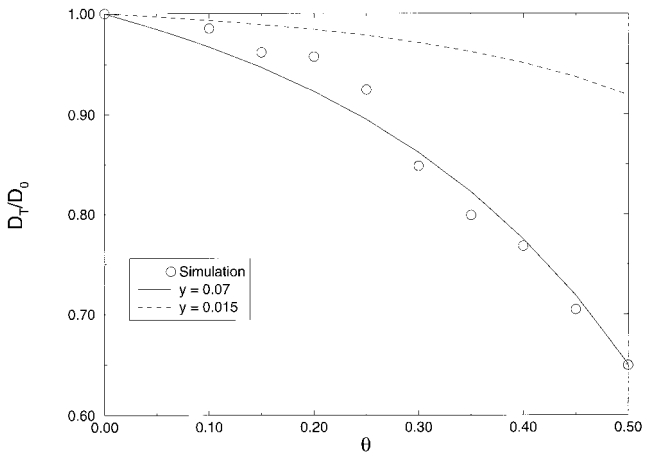

FIGURE 14 Relative diffusion coefficient, D_T/D_0, where D_0 is the zero-coverage surface diffusion coefficient, against surface coverage for $I = 0.3$ M. The solid and dashed lines show Minton's model (Eq. 9).

CONCLUSION

We have examined the effects of lateral mobility and interparticle interactions on lysozyme adsorption kinetics, using BD simulations. The results discussed in the previous section show that the adsorption is strongly influenced by double-layer screening effects, which is consistent with an experimental study of lysozyme adsorption on silicon oxide surfaces (Wahlgren et al., 1995). Similar results are available for other systems (Ramsden and Prenosil, 1994). Unlike the studies of Haggerty and Lenhoff (1993), we do not observe the formation of extended arrays of molecules on the surface. There is evidence, however, for localized clustering at high salt concentrations. The asymptotic kinetics are consistent with $1/\ln(t)$ behavior (Privman and Barma, 1992), but also with a power law. Significantly longer runs with a simpler potential may be able to distinguish between these two kinetics.

The simulations show that mobility of the adsorbed proteins enhances the surface coverage compared with strictly localized adsorption (RSA), leading to an increased rate of adsorption. There is some evidence for increased order in the adsorbed layer with decreasing bulk concentration. This result is in qualitative agreement with the study of Ramsden et al. (1994), but we do not observe the extended validity of the Langmuir kinetics, as was observed by these authors and described by them as due to enhanced clustering at low bulk concentrations.

The lateral diffusion coefficients, calculated from mean squared displacement, decrease with increasing surface coverage, as in the theoretical model of Minton (1989). Tilton et al. (1990a) calculated the long-time diffusion coefficient of irreversibly adsorbed bovine serum albumin on poly(methylmethacrylate) and found that it decreased by approximately one order of magnitude as θ increased from 0.1 to 0.7. As far as we know, this was the first experimental study to calculate the diffusion coefficient over a wide range of surface coverage. The presence of both individual molecules and clusters, seen in the high surface coverage configurations for high ionic strength, is consistent with the idea of mobile (single molecules) and immobile fractions (clusters) proposed by Tilton (1998). Other possible mech-

anisms for heterogeneous diffusion include orientational and conformational effects that are not present in the current model.

Modeling protein adsorption is a challenging and difficult endeavor for reasons already mentioned. The simple spherical charge model used in this study has already been successfully used to model lysozyme (Oberholzer et al., 1997b; Roth and Lenhoff, 1993; Roth et al., 1998) and to understand the different energy contribution involved in lysozyme adsorption (Roth and Lenhoff, 1993; Roth et al., 1998). But there are certain limitations: the model cannot be used to understand the conformational changes (Robeson and Tilton, 1996; Asthagiri and Lenhoff, 1997) that accompany the adsorption process. The spherical shape and uniform charge assumption will also break down when the protein is significantly nonspherical with an anisotropic charge distribution (Asthagiri and Lenhoff, 1997). Currently we are developing models incorporating shape and charge anisotropy to study protein adsorption at infinite dilution.

APPENDIX A: POTENTIAL MODEL

The electrostatic interaction energy is assumed to consist of a pairwise sum of protein-protein (pp) terms of the form

$$U_{pp}^{el}(r) = \frac{B_{pp}}{r}\exp[-\kappa a(r-2)] \tag{A1}$$

where a is the particle radius and r is the center-center distance between the adsorbed particles expressed in units of a. The influence of the electrolyte concentration on the interaction is incorporated into the model, using the Debye parameter, κ, which is proportional to the square root of the ionic strength, I.

The Yukawa coefficient B_{pp} is obtained using a superposition approximation (Sader, 1997) and is given as follows:

$$B_{pp} = \left(\frac{4\pi kT\epsilon\epsilon_0 a}{e^2}\right)\left(\frac{\psi_p + 4\gamma\Omega\kappa a}{1+\Omega\kappa a}\right)^2 \tag{A2}$$

where ϵ is the dielectric constant of the solution, ϵ_0 is the dielectric permittivity of free space, e is the electronic charge, k is Boltzmann's constant, and T is the absolute temperature. ψ_p represents the electrostatic potential of the particle, and γ and Ω are given by

$$\gamma = \tanh\left(\frac{\psi_p}{4}\right) \quad \text{and} \quad \Omega = \left(\frac{\psi_p - 4\gamma}{2\gamma^3}\right)$$

Note that ψ_p is scaled by kT/e and is a dimensionless quantity. It can be obtained as follows (Sader, 1997):

$$\sigma_s^* = \psi_p + \frac{\psi_p}{\kappa a} - \frac{{\tau_1}^2\kappa a}{\tau_2 - \tau_1\kappa a} \tag{A3}$$

where $\sigma_s^* = e\sigma_s/(\kappa\epsilon_0\epsilon kT)$ is the reduced surface charge density and σ_s is related to the net charge of the protein by $\sigma_s = Ze/4\pi a^2$. The quantities τ_1 and τ_2 are given by

$$\tau_1 - 2\sinh\left(\frac{\psi_s}{2}\right) - \psi_s \quad \tau_2 = 4\sinh\left(\frac{\psi_p}{4}\right) - \psi_p$$

The van der Waals interaction energy is also assumed to be a pairwise sum of protein-protein terms:

$$U_{pp}^{vdw}(r) = \frac{A_{pp}}{6kT}\left[\frac{2}{r^2-4} + \frac{2}{r^2} + \ln\left(1 - \frac{4}{r^2}\right)\right] \tag{A4}$$

The Hamaker constant (Hunter, 1992), A_{pp}, which characterizes the interaction between particles in the presence of an intervening medium, is chosen to be 2×10^{-20} J (Hunter, 1992).

Finally, the repulsive interaction between protein molecules is modeled using a short-range form,

$$U_{pp}^{rep}(r) = \frac{f}{(r-2)^g} \tag{A5}$$

where f and g are constants with values of 4×10^{-7} and 6, respectively. This repulsive interaction is essential for stabilizing the system of proteins, particularly at high ionic strength (Oberholzer et al., 1997b).

APPENDIX B: RELATION BETWEEN INSERTION INTERVAL AND BULK CONCENTRATION

At zero coverage the rate of adsorption is given by

$$\frac{\Delta\theta}{\Delta t} = \frac{\pi a^2}{\Delta t L^2 n_{ins}} = k_a c \tag{B1}$$

The time interval between two insertions is given by

$$\Delta t = n_{ins}\delta t \tag{B2}$$

where δt is the BD time step. Combining Eqs. B2 and B3 leads to

$$n_{ins} = \frac{\pi a^2}{L^2\Delta t k_a c} \tag{B3}$$

which shows that the bulk concentration is inversely related to the insertion interval, n_{ins}.

We thank Abraham Lenhoff and Mathew Oberholzer for sending preprints of their work on colloidal adsorption.

We thank the National Science Foundation for financial support.

REFERENCES

Adamczyk, Z., B. Siwek, M. Zembala, and P. Belouschek. 1994. Kinetics of localized adsorption of colloid particles. *Adv. Colloid Interface Sci.* 48:151–280.

Andrade, J. D. 1985. Surface and Interfacial Aspects of Biomedical Polymers, Vol. 2, Protein Adsorption. Plenum, New York.

Andrade, J. D., and V. Hlady. 1986. Protein adsorption and materials biocompatibility: a tutorial review and suggested hypotheses. *Adv. Polym. Sci.* 79:1–63.

Ansell, C. G., and E. Dickinson. 1985. Aggregate structure and coagulation kinetics in a concentrated dispersion of interacting colloidal particles. *Chem. Phys. Lett.* 122:594–598.

Asthagiri, D., and A. M. Lenhoff. 1997. Influence of structural details in modelling electrostatically driven protein adsorption. *Langmuir*. 13: 6761–6768.

Bafaluy, J., B. Senger, J. C. Voegel, and P. Schaaf. 1993. Effect of hydrodynamic interaction on the distribution of adhering Brownian particles. *Phys. Rev. Lett.* 70:623–626.

Bauer, D., E. Dillmann, and W. Jaeger. 1998. Adsorption of poly (diallyedimethyl-ammonium chloride) (PDADMAC) and of copolymers of DADMAC with *N*-methyl-*N*-vinyl-acetamide (NMVA) on colloidal silica. *Prog. Colloid Polym. Sci.* 109:161–169.

Billsten, P., U. Carlsson, and H. Elwing. 1998. Studies on the conformation of adsorbed proteins with the use of nanoparticle technology. *In* Biopolymers at Interfaces, Surfactant Science Series. Marcel Dekker, Inc., New York, NY. 627–650.

Burghardt, T. P., and D. Axelrod. 1981. Total internal reflection/fluorescence photobleaching recovery study of serum albumin adsorption studies. *Biophys. J.* 33:455–467.

Chan, V., D. J. Graves, P. Fortina, and S. E. McKenzie. 1997. Adsorption and surface diffusion of DNA oligonucleotides at liquid/solid interfaces. *Langmuir.* 13:320–329.

Ermak, D. L., and J. A. McCammon. 1978. Brownian dynamics with hydrodynamic interactions. *J. Chem. Phys.* 69:1352–1360.

Feder, J., and I. Giaever. 1980. Adsorption of ferritin. *J. Colloid Interface Sci.* 78:144–154.

Haggerty, L., and A. M. Lenhoff. 1993. Analysis of ordered arrays of adsorbed lysozyme by scanning tunnelling microscopy. *Biophys. J.* 64:886–895.

Horbett, T. A., and J. L. Brash, editors. 1995. Proteins at Interfaces. II. Fundamentals and Applications. ACS Symposium Series. ACS, Washington, D.C. 602.

Horsley, D., J. Herron, V. Hlady, and J. D. Andrade. 1991. Fluorescence quenching of adsorbed hen and human lysozymes. *Langmuir.* 7:218–222.

Hunter, R. J. 1992. Foundations of Colloid Science, Vol. 1. Clarendon Press, Oxford.

Johnson, C. A., P. Wu, and A. M. Lenhoff. 1994. Electrostatic and van der Waals contributions to protein adsorption. 2. Modelling of ordered arrays. *Langmuir.* 10:3705–3713.

Kondo, A., S. Oku, and K. Higashitani. 1991. Structural changes in protein molecules adsorbed on ultrafine silica particles. *J. Colloid Interface Sci.* 143:214–221.

Langmuir, I. 1918. The adsorption of gases on plane surfaces of glass, mica and platinum. *J. Am. Chem. Soc.* 40:1361–1403.

Lim, K., and J. N. Herron. 1991. Biomedical Applicaitons of Polyethylene Glycol Chemistry. J. M. Harris, editor. Plenum, New York.

Lu, D. R., S. J. Lee, and K. Park. 1991. Calculation of solvation interaction energies for protein adsorption on polymer surfaces. *J. Biomater. Sci. Polym. Ed.* 3:127–147.

Lu, D. R., and K. Park. 1990. Protein adsorption on polymer surfaces: calculation of adsorption energies. *J. Biomater. Sci. Polym. Ed.* 4:243–260.

MacRitchie, F. 1978. Proteins at interfaces. *Protein Chem.* 32:283–326.

Michaeli, I., D. R. Absolom, and C. J. Van Oss. 1980. Diffusion of adsorbed protein within the plane of adsorption. *J. Colloid Interface Sci.* 77:586–587.

Minton, A. P. 1989. Lateral diffusion of membrane proteins in protein-rich membranes. *Biophys. J.* 55:805–808.

Norde, W., and J. Lyklema. 1978. The adsorption of human plasma albumin and bovine pancreas ribonuclease at negatively charged polystyrene surfaces. 1. Adsorption istotherms, effects of charge, ionic strength and temperature. *J. Colloid Interface Sci.* 66:257–265.

Nygren, N., and M. Stenberg. 1990. Surface-induced aggregation of ferritin at a liquid-solid interface. *Prog. Colloid Polym. Sci.* 82:15–18.

Oberholzer, M. R., J. M. Stanksvich, S. L. Carnie, D. Y. C. Chan, and A. M. Lenhoff. 1997a. 2D and 3D interactions in random sequential adsorption of charged particles. *J. Colloid Interface Sci.* 194:138–153.

Oberholzer, M. R., N. J. Wagner, and A. M. Lenhoff. 1997b. Grand canonical Brownian dynamics simulation of colloidal adsorption. *J. Chem. Phys.* 107:9157–9167.

Pagonabarraga, I., and J. M. Rubi. 1994. Influence of hydrodynamic interactions on the adsorption process of large particles. *Phys. Rev. Lett.* 73:114–117.

Pink, D. A. 1985. Protein lateral movement in lipid bilayers. Simulation studies of its dependence upon protein concentration. *Biochim. Biophys. Acta.* 818:200–204.

Pomeau, Y. 1980. Some asymptotic estimates in the random parking problem. *J. Phys. A.* 13:L193–L196.

Privman, V., and M. Barma. 1992. Random sequential adsorption on a line: mean-field theory of diffusional relaxation. *J. Chem. Phys.* 97: 6714–6719.

Ramsden, J. J. 1993. Concentration scaling of protein deposition kinetics. *Phys. Rev. Lett.* 71:295–298.

Ramsden, J. J. 1995. Puzzles and paradoxes in protein adsorption. *Chem. Soc. Rev.* 24:73–78.

Ramsden, J. J., G. I. Bachamanova, and A. I. Archakov. 1994. Kinetic evidence for protein clustering at a surface. *Phys. Rev. E.* 50:5072–5076.

Ramsden, J. J., and J. E. Prenosil. 1994. Effect of ionic strength on protein adsorption kinetics. *J. Phys. Chem.* 98:5376–5381.

Rényi, A. 1958. Egy egydimenziós véletlen térkitöltési problémától. *Publ. Math. Inst. Hung. Acad. Sci.* 3:109–125.

Robeson, J. L., and R. D. Tilton. 1996. Spontaneous reconfiguration of adsorbed lysozyme layers observed by total internal reflection fluorescence with a pH-sensitive fluorophore. *Langmuir.* 12:6104–6113.

Roth, C. M., and A. M. Lenhoff. 1993. Electrostatic and van der Waals contributions to protein adsorption: computation of equilibrium constants. *Langmuir.* 9:962–972.

Roth, C. M., J. E. Sader, and A. M. Lenhoff. 1998. Electrostatic contribution to the energy and entropy of protein adsorption. *J. Colloid Interface Sci.* 203:218–221.

Sader, J. E. 1997. Accurate analytic formulae for the far field effective potential and surface charge density of a uniformly charged sphere. *J. Colloid Interface Sci.* 188:508–510.

Schaaf, P., and J. Talbot. 1989a. Kinetics of random sequential adsorption. *Phys. Rev. Lett.* 62:175–177.

Schaaf, P., and J. Talbot. 1989b. Surface exclusion effects in adsorption processes. *J. Chem. Phys.* 91:4401–4409.

Schmitt, A., R. Varoqui, S. Uniyal, J. L. Brash, and C. Pusineri. 1983. Interaction of fibrinogen with solid surfaces of varying charge and hydrophobic-hydrophilic balance. 1. Adsorption isotherms. *J. Colloid Interface Sci.* 92:25–34.

Shibata, C. T., and A. M. Lenhoff. 1992. TIRF of salt and surface effects on protein adsorption. 1. Equilibrium. *J. Colloid Interface Sci.* 148: 469–484.

Swendsen, R. H. 1981. Dynamics of random sequential adsorption. *Phys. Rev. A.* 24:504–508.

Tarjus, G., P. Schaaf, and J. Talbot. 1990. Generalized random sequential adsorption. *J. Chem. Phys.* 93:8352–8360.

Tilton, R. D. 1998. Mobility of biomolecules at interfaces. *Surfactant Sci. Ser.* 75:363–408.

Tilton, R. D., A. P. Gast, and C. R. Robertson. 1990a. Surface diffusion of interacting proteins. Effect of concentration on the lateral mobility of adsorbed bovine serum albumin. *Biophys. J.* 58:1321–1326.

Tilton, R. D., C. R. Robertson, and A. P. Gast. 1990b. Lateral diffusion of bovine serum albumin adsorbed at the solid-liquid interface. *J. Colloid Interface Sci.* 137:192–203.

Verway, E. J. W., and J. Th. G. Overbeek. 1948. Theory of the Stability of Lyophobic Colloids. Elsevier, Amsterdam.

Wahlgren, M., T. Arnebrant, and I. Lundström. 1995. The adsorption of lysozyme to hydrophilic silicon oxide surfaces: comparison between experimental data and models for adsorption kinetics. *J. Colloid Interface Sci.* 175:506–514.